ELSEVIER

Chemical Physics 219 (1997) 333–340

Chemical Physics

Fluorescence excitation spectroscopy of some haloethenes, $CF_2=CXY$ ($XY \equiv FCl, Cl_2, FH$), excited in the vacuum ultraviolet (70–180 nm)

M. Ahmed [a], C.J. Apps [a], M.J. Bramwell [a], J.L. Cooper [a], C. Hughes [a], K. Reinhardt [a], J.C. Whitehead [a,*], F. Winterbottom [a], A. Hopkirk [b]

[a] *Department of Chemistry, University of Manchester, Manchester, M13 9PL UK*
[b] *CLRC Daresbury Laboratory, Daresbury, Warrington, Cheshire WA4 4AD UK*

Received 3 February 1997; accepted 11 April 1997

Abstract

The fluorescence excitation spectra for three haloethenes, C_2F_3H, C_2F_3Cl and $C_2F_2Cl_2$, have been measured in a molecular beam using synchrotron radiation in the range 70–180 nm as the excitation source. These results extend previous studies on the fluorescence excitation spectrum for C_2F_3Cl to shorter wavelengths (< 105 nm) and present the first such results for C_2F_3H and $C_2F_2Cl_2$. The spectra show a series of well defined Rydberg progressions converging to the first and second ionisation potentials superimposed upon continuous and broadly structured features that correspond to valence transitions. Vibrational structure is seen for features at energies below the first ionisation potential but not above. As no absorption spectra have been reported for these molecules for wavelengths less than ≈ 105 nm, the spectra are analysed with reference to photoelectron and electron impact spectroscopic studies on these molecules. © 1997 Elsevier Science B.V.

1. Introduction

The study of the vacuum ultraviolet spectroscopy of haloethenes allows comparison to be made with corresponding studies for ethene. For wavelengths > 105 nm, the vacuum ultraviolet absorption spectra of ethene and its halogen-substituted derivatives show a variety of electronic transitions, e.g. valence excitations from the highest occupied π-orbital to the unoccupied π^*-orbital ($V \leftarrow N$) or to Rydberg states ($R \leftarrow N$) often with associated vibrational progressions and, in the case of the haloethenes, additional features due to excitations of halogen lone-pair orbitals. (This notation comes from Merer and Mulliken [1] where N is the normal state (electronic ground state), V is the lowest excited singlet state and R represents the Rydberg states). The non-bonding halogen orbitals can be oriented perpendicular or parallel to the plane of the molecule. The out-of-plane orbital can interact with the π orbitals creating new orbital combinations and the inductive effects due to the electronegativity of the halogen atoms can stabilise or destabilise the orbitals compared to ethene causing shifts in the band positions. The study of the effects of halogen substitution allows one to investigate the effect of different halogen atoms on the electronic structure of ethene. Robin has comprehensively reviewed the VUV spectroscopy of haloethylenes [2]. The results of vacuum ultraviolet absorp-

* Corresponding author. Fax: 44 161 2754598

PII S0301-0104(97)00114-6

tion [3–5], fluorescence excitation [6], photoelectron [7–10] and electron-impact spectroscopy [11] provide complementary information from which an insight into the electronic structure of the haloethenes can be obtained.

In this paper, we report studies of the fluorescence excitation spectroscopy of a molecular beam of three related haloethenes (C_2F_3H, C_2F_3Cl and $C_2F_2Cl_2$) excited by vacuum ultraviolet synchrotron radiation in the wavelength range 70–180 nm by detecting the fluorescence from the electronically-excited photofragments, CF_2^* and CXY^*. The fluorescence excitation spectrum is related to the absorption spectrum and in regions of reasonably constant fluorescence quantum yield (the ratio of the fluorescence cross section to the absorption cross section), the two spectra are similar and contain the same information. Fluorescence excitation spectroscopy may also give additional information about the nature of the states involved in a transition from the identity of the photofragments. The use of a molecular beam results in enhanced fluorescence signal levels because the collision-free conditions of the beam eliminate the collisional quenching that can reduce the level of fluorescence in a conventional cell experiment [12]. Because of technical limitations, most optical studies (absorption and fluorescence excitation) of the vacuum ultraviolet spectroscopy of the haloethenes have been restricted to a lower wavelength of ≈ 105 nm. Nee et al. [6] have measured the fluorescence excitation spectrum of C_2F_3Cl in the excitation region 106–230 nm. Scott and Russell [3,4] and Bélanger and Sandorfy [5] have measured the absorption spectra for C_2F_3Cl, C_2F_3H and $C_2F_2Cl_2$ for wavelengths down to ≈ 115 nm. The only studies for haloethenes at shorter wavelengths are those of the absorption spectra of the isomers of C_2H_2FCl [13] and C_2F_2HCl [14] which extend to wavelengths of 50 nm, corresponding to an excitation energy of 25 eV. There are no reported absorption spectra for wavelengths less than ≈ 105 nm for C_2F_3Cl, C_2F_3H and $C_2F_2Cl_2$.

2. Experimental

The experimental arrangement is similar to that used previously by us in a study of the fluorescence excitation of a molecular beam of ND_3 excited by vacuum ultraviolet synchrotron radiation [12]. The experiments were performed in a stainless steel molecular beam chamber pumped by a 2.5 $m^3\ s^{-1}$ cryopump sited directly opposite the beam source. The molecular beam source consisted of a stainless steel nozzle of 0.18 mm diameter which could be heated to prevent condensation. The haloethylene gas was admitted undiluted to the beam source via a mass controller to give a stagnation pressure of ≈ 100–400 Torr. The VUV radiation of the synchrotron (Daresbury SRS, station 3.1), operating in multibunch mode, was dispersed by a 1 m Seya Namioka monochromator with an effective resolution of ≈ 2 Å scanned with a step size of 1 Å. The radiation entered the chamber via a quartz capillary tube and intersected the molecular beam close to the nozzle. The resulting fluorescence was observed at right angles to both the synchrotron and molecular beam directions via a MgF_2 window and filter by a pulse counting photomultiplier (EMI 9883QKA; 200–600 nm spectral response). Colour glass filters (Schott WG230, WG360 or GG385) were used to spectrally identify the fluorescence. Spectra were recorded using either the bare photomultiplier or in conjunction with a cut-in colour glass filter. In this way, by differencing, $\tilde{A} \rightarrow \tilde{X}$ fluorescence from electronically-excited CF_2^* (200 or 230–360 nm) could be crudely separated from that resulting from $CFCl^*$, CCl_2^* or CHF^* (> 360 or 385 nm). The fluorescence signals were corrected for any variation in the intensity of the synchrotron radiation with time and wavelength.

The haloethylenes were used as supplied by the manufacturers (C_2F_3Cl, Matheson; C_2F_3H and $C_2F_2Cl_2$, Fluorochem).

3. Results and discussion

The fluorescence excitation spectra for C_2F_3H, C_2F_3Cl and $C_2F_2Cl_2$ are shown in Figs. 1–6 for two spectral regions, 105–180 nm and ≈ 70–120 nm. The assignment of the various valence ($V \leftarrow N$) and Rydberg ($R \leftarrow N$) transitions at energies below the first ionisation potentials come from the appropriate absorption spectra [3–5]. The results for the two

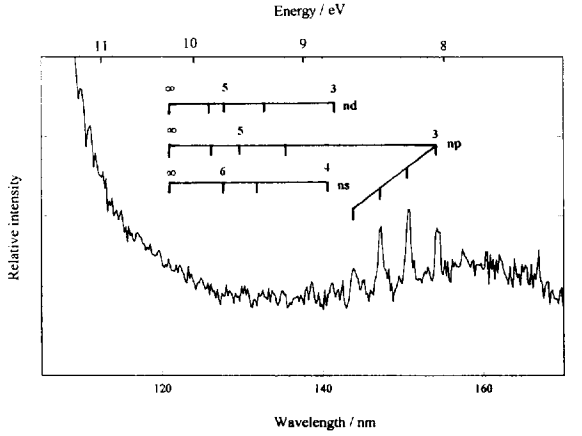

Fig. 1. The fluorescence excitation spectrum of C_2F_3H in the spectral region 110–180 nm. The fluorescent emission in the range 360–600 nm was attributed to emission from electronically-excited CHF^*; no emission was observed in the range 200–360 nm that could be attributed to electronically-excited CF_2^*. The assignments come from Bélanger and Sandorfy [5].

different spectral regions will be discussed separately. These two regions correspond broadly to energies above and below the first ionisation limit.

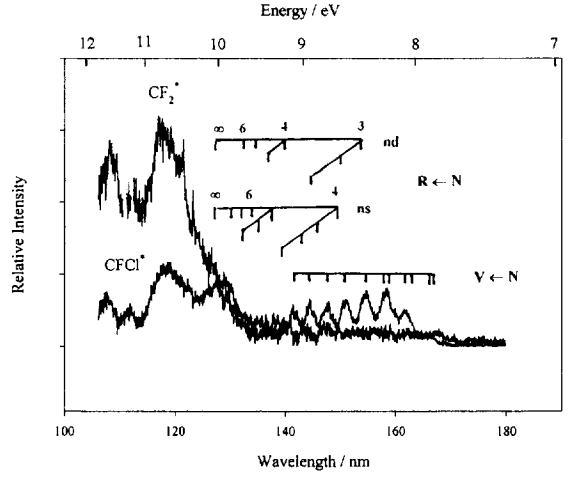

Fig. 2. The fluorescence excitation spectrum of C_2F_3Cl in the spectral region 105–180 nm. The fluorescent emission in the range 360–600 nm was attributed to emission from electronically-excited $CFCl^*$; that in the range 200–360 nm to electronically-excited CF_2^*. The assignments come from Scott and Russell [3,4].

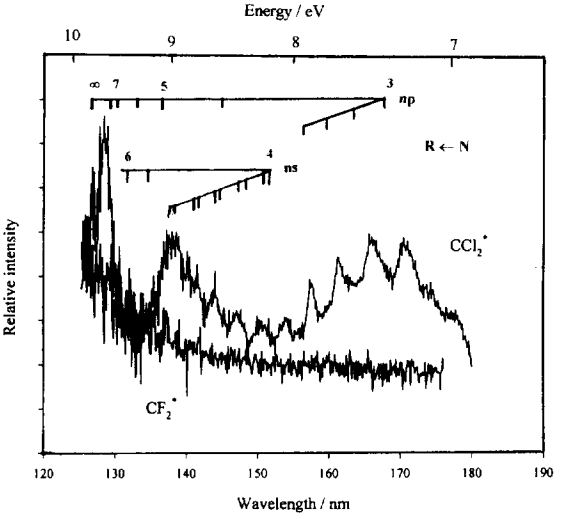

Fig. 3. The fluorescence excitation spectrum of $C_2F_2Cl_2$ in the spectral region 125–180 nm. The fluorescent emission in the range 360–600 nm was attributed to emission from electronically-excited CCl_2^*; that in the range 200–360 nm to electronically-excited CF_2^*. The assignments come from Scott and Russell [3,4].

3.1. 105–180 nm (7–12 eV)

The fluorescence excitation spectra of all three molecules in this region show a very close similarity with the corresponding absorption spectra [3–5] and, in the case of C_2F_3Cl, with the previously reported fluorescence excitation spectrum [6]. The transitions in this region are mainly due to transitions from the ground state π orbital (N) to the singlet π^* valence state (V ← N) or to Rydberg states (R ← N). For C_2F_3Cl, the V ← N transition consists of a broad continuum overlaid by vibrational structure associated mainly with stretching of the C=C bond. Vibrational structure is associated with the R ← N transition in all cases. The Rydberg series converge to a limit at the first ionisation potential ($\approx$ 122 nm for C_2F_3H; $\approx$ 127 nm for C_2F_3Cl; $\approx$ 126 nm for $C_2F_2Cl_2$). For $C_2F_2Cl_2$ and C_2F_3Cl, an additional transition is seen at $\approx$ 139 nm and $\approx$ 129 nm, respectively, identified as CCl_2^* or CF_2^* emission which is assigned to excitation of a 4s ← 3p transition associated with orbitals localised on a chlorine atom. The peak at $\approx$ 118 nm for C_2F_3Cl which is seen in both CF_2^* and $CFCl^*$ emission corresponds to excitation of higher chlorine atomic Rydbergs.

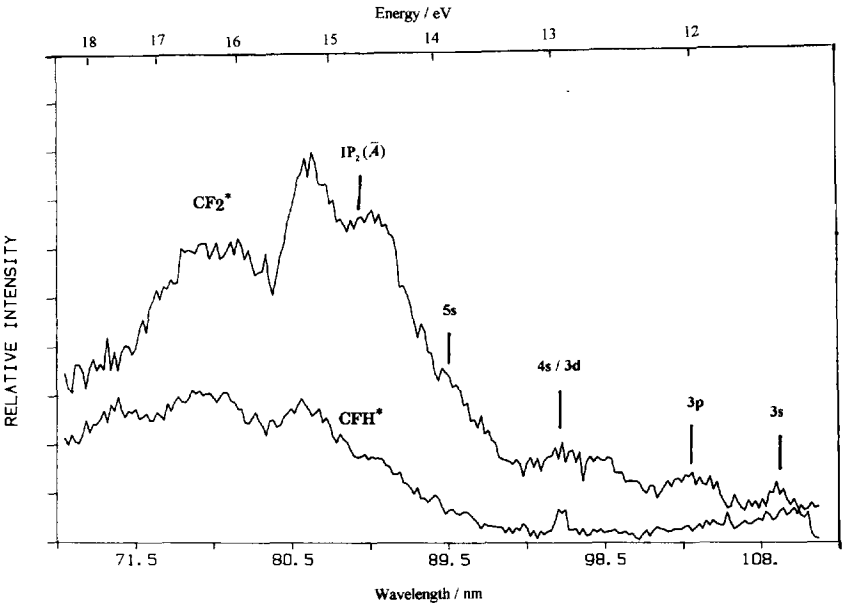

Fig. 4. The fluorescence excitation spectrum of C_2F_3H in the spectral region 67–110 nm. The fluorescent emission in the range 360–600 nm was attributed to emission from electronically-excited CHF*; that in the range 200–360 nm to electronically-excited CF_2^*. See the text for a discussion of the assignments.

The observed and the calculated thermodynamic wavelength thresholds for the various dissociation channels

$$CF_2{=}CXY + h\nu \rightarrow CF_2 + CXY \quad (1)$$

$$CF_2{=}CXY + h\nu \rightarrow CF_2 + CXY^* \quad (2)$$

$$CF_2{=}CXY + h\nu \rightarrow CF_2^* + CXY \quad (3)$$

$$CF_2{=}CXY + h\nu \rightarrow CF_2^* + CXY^* \quad (4)$$

are listed in Table 1. In all cases, the observed threshold for the formation of electronically-excited photofragments via channels (2) and (3) is at higher energy than the asymptotic thermodynamic thresholds, indicating that either the dissociating state of $CF_2{=}CXY$ lies at much higher energies than the photofragments or that there is a large barrier to dissociation. Thermodynamically, for C_2F_3H, none of the fluorescence observed in this region can be associated with channel (4) in which both photofragments are electronically-excited, whereas it is possi-

Table 1
The calculated thermodynamic wavelength thresholds for the various dissociation channels; the experimentally observed values are given in parentheses

		Wavelength threshold (nm)		
		$CF_2{=}CFH$	$CF_2{=}CFCl$	$CF_2{=}CCl_2$
$CF_2{=}CXY + h\nu \rightarrow$	$CF_2 + CXY$	394.2	410.8	279.5
	$CF_2 + CXY^*$	199.0 (170.0)	201.4 (170.0)	248.0 (180.0)
	$CF_2^* + CXY$	142.0 (108.0)	162.4 (134.6)	165.0 (150.0)
	$CF_2^* + CXY^*$	114.0	115.2	129.0

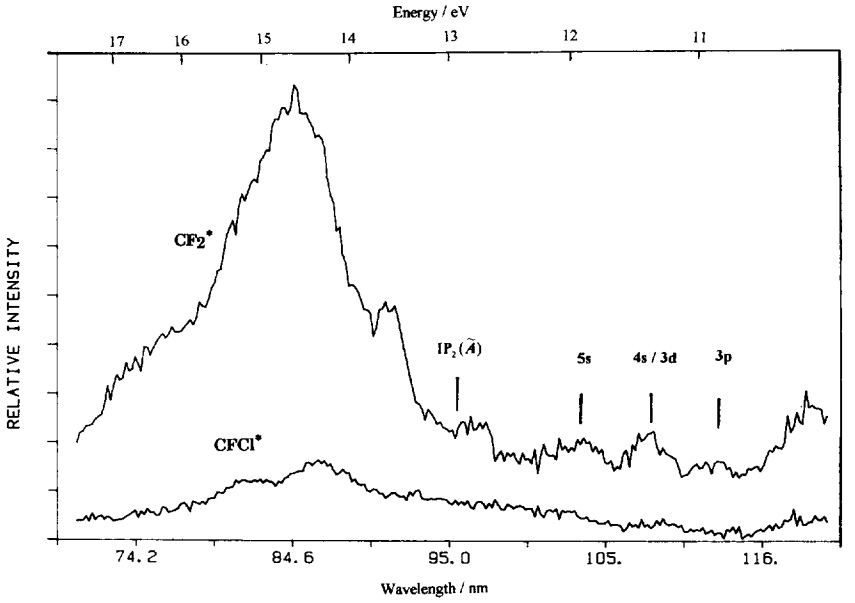

Fig. 5. The fluorescence excitation spectrum of C_2F_3Cl in the spectral region 70–120 nm. The fluorescent emission in the range 360–600 nm was attributed to emission from electronically-excited CFCl*; that in the range 200–360 nm to electronically-excited CF_2^*. See the text for a discussion of the assignments.

ble that some of the shorter wavelength features for C_2F_3Cl and $C_2F_2Cl_2$ in which emission is seen for both photofragments may come from channel (4). However, given the differences between the calculated and observed thresholds noted for channels (2) and (3), it is likely that these features (e.g. the peak

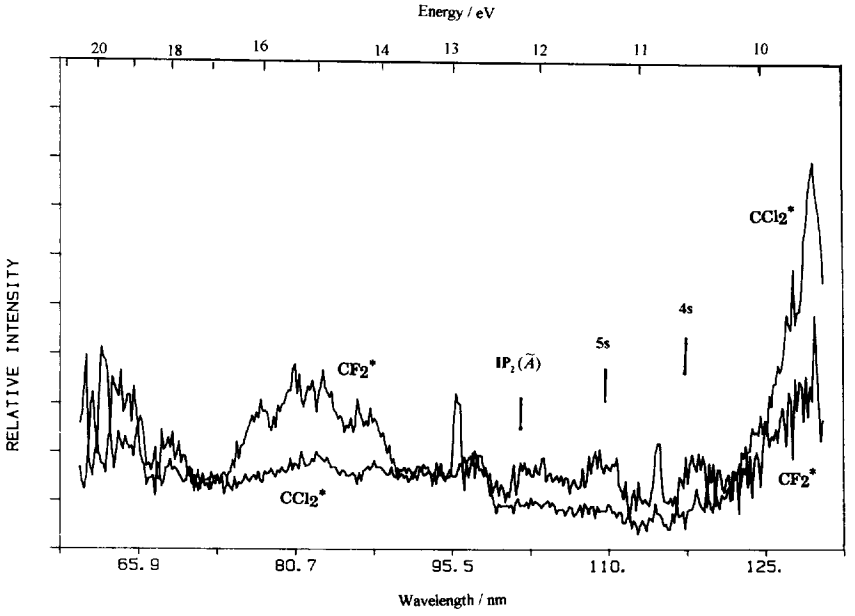

Fig. 6. The fluorescence excitation spectrum of $C_2F_2Cl_2$ in the spectral region 70–130 nm. The fluorescent emission in the range 360–600 nm was attributed to emission from electronically-excited CCl_2^*; that in the range 200–360 nm to electronically-excited CF_2^*. See the text for a discussion of the assignments.

at ≈ 118 nm for C_2F_3Cl) represent a branching between channels (2) and (3) rather than the simultaneous production of two electronically-excited photofragments.

When determining the relative branching between the photofragments, CF_2^* and CXY^*, from the fluorescence excitation spectra, it is necessary to take into account the relative transition probabilities for the different electronically-excited halocarbene species. This can be estimated from the radiative lifetimes of the $\tilde{A}$ states which range from 0.06 μs for CF_2^*, 0.64 μs for $CFCl^*$, 2.45 μs for CHF^* to 3.8 μs for CCl_2^* [15–17]. These values indicate that, all other things being equal, emission from CF_2^* will be expected to be more intense than that from CXY^* by a factor of ≈ 10 for C_2F_3Cl, ≈ 40 for C_2F_3H and ≈ 60 for $C_2F_2Cl_2$. The molecular beam environment in which these experiments are conducted favours the detection of short-lived emitters compared with longer-lived species which can be carried out of the observation region in the beam. However, we have estimated [18] that under the present conditions, all species with lifetimes less than 10 μs are optimally detected. These factors indicate that for all the systems studied the channel producing CF_2^* has a smaller branching ratio than that for CXY^*. In their synchrotron studies on the fluorescence from photoexcitation of C_2F_3Cl in this spectral region, Nee et al. [6] did not disperse the fluorescence in any way and were thus unable to distinguish between emission from CF_2^* and $CFCl^*$. However using an atomic line source at 155 nm, they were able to spectrally disperse the fluorescence and show that the $CFCl^*$ produced at this wavelength is vibrationally-excited although the extent of the vibrational excitation was not determined.

3.2. 70–105 nm (12–18 eV)

In this region, we can identify Rydberg states that converge to the second ionisation potential of the haloethenes corresponding to the production of the first electronically-excited state ($\tilde{A}$) of the $C_2F_2XY^+$ ion. Corresponding features have been reported in the photoabsorption spectrum of ethene [19] and of 2-chloro-1,1-difluoroethene [14]. For C_2F_3H and C_2F_3Cl, the Rydberg states have been assigned with reference to the electron-impact spectroscopy of these molecules by Coggiola et al. [11] where the corresponding features were observed. For $C_2F_2Cl_2$, the features at ≈ 110 and 117 nm were assigned to 5s and 4s Rydberg states by using the same quantum defect values derived by Scott and Russell [3] for the Rydberg series converging to the first ionisation potential. In contrast to the vibrational structure in the first ionisation band ($\tilde{X}$) observed by photoelectron spectroscopy, such studies show no resolvable vibrational structure associated with the second band ($\tilde{A}$) seen for the present haloethenes, except for $C_2F_2Cl_2$ [7–10]. Thus, we would not anticipate any vibrational structure to be associated with the Rydberg progressions converging on the second ionisation potential in our fluorescence excitation spectra assuming that there are geometrical similarities between the $\tilde{A}$ states of the ions and the Rydberg states of the molecules, where similar orbital excitations are involved.

For all three haloethenes studied, there is considerable fluorescent intensity at excitation energies above the second ionisation potentials, IP_2 ($\tilde{A}$) as can be seen in Figs. 4–6. For C_2F_3H and C_2F_3Cl, these features are more intense than those at longer wavelengths, whereas for $C_2F_2Cl_2$, they are much weaker. For C_2F_3H, the peak at ≈ 81.5 nm (Fig. 4) corresponds to a feature discernible in the electron-energy loss spectrum at $\Delta E \approx 15.2$ eV [11]. For C_2F_3Cl, the electron-energy loss studies show peaks at $\Delta E \approx$ 14.3 and 15.5 eV which would predict the existence of corresponding features at 80 and 86.7 nm in the fluorescence excitation spectrum (Fig. 5). In this region we observe a peak in the CF_2^* emission at 84.9 nm and two peaks in the $CFCl^*$ emission at 81.7 and 86.2 nm. The latter two peaks would seem to accord most closely to the electron-energy loss results. It is not easy to readily assign any of the features lying above the second ionisation potential to Rydberg states converging to higher ionic states and it has been suggested [11] that they may correspond to excitation of valence σ orbitals e.g. $\sigma^* \leftarrow \sigma$ transitions.

4. Conclusions

All of the fluorescence excitation spectra for the haloethenes studied show a similar structure. Series of Rydberg transitions are superimposed on continu-

ous and broadly structured features associated with valence transitions. Rydberg progressions can be identified converging to both the first and second ionisation potentials of the haloethenes, but not for higher ionisation states. Vibrational structure is seen for transitions below the first ionisation potential but not above, in line with the observations of photoelectron spectroscopy [7–10]. This is in contrast to the photoabsorption studies for some chlorodifluoroethenes [14] which do show vibrational structure in the Rydberg progressions converging to the second ionisation potential and to the photoelectron spectroscopy for monochlorofluoroethenes [13] and difluoroethenes [8,9] which show vibrational structure associated with the higher ionisation bands. The vibrational structure below the first ionisation potential is mainly associated with C=C stretching and suggests that the excited state involved in the transition is formed with a highly extended C=C bond. The excitations observed at energies above the first ionisation potential probably involve little geometrical change upon excitation.

From the energies of the bands observed in the photoelectron spectra [7–10] and from the positions of the maxima of the $\pi \rightarrow \pi^*$ valence transitions and the position of the Rydberg and chlorine 'atomic' transitions seen in photoabsorption and fluorescence spectra [3–6], it is possible to construct orbital energy level diagrams for these molecules. The resulting diagrams are given in Fig. 7 with the assignments of the orbitals as given by the photoelectron studies [7–10]. It can be seen that there is a destabilisation of both the π and π^* orbitals upon removal of the chlorine atoms in going across the sequence from C_2F_3H to $C_2F_2Cl_2$. This is an example of the inductive effect that has previously been noted upon the addition of chlorine atoms to haloethylenes [13]. The assignment of Rydberg transitions converging on the second ionisation potentials in the fluorescence excitation spectra based on the results from electron-impact spectroscopy [11] is confirmed by the diagram. It is possible to roughly predict the maxima in the valence transitions from the diagrams and there are likely transitions that might explain the broad maxima seen in the region 70–90 nm. Many of the possible transitions originate from excitations of inner σ orbitals, but there is insufficient information to make these assignments uniquely. Further information might result from more detailed molecular orbital calculations that included transition probabilities for the possible excitations and measurement of the polarisation of the fluorescence emission to aid in the identification of the symmetries of the states involved. Measurement of the photoabsorption

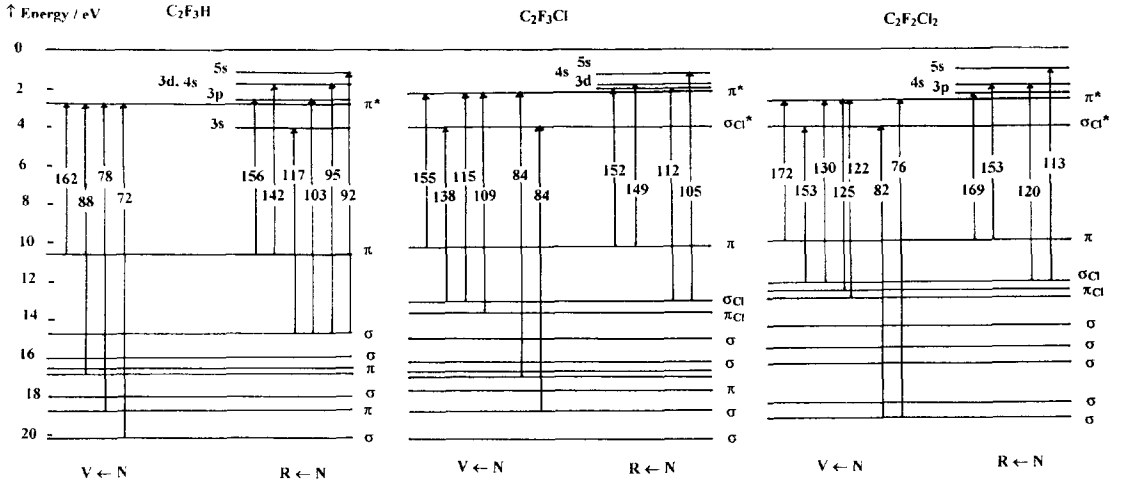

Fig. 7. Approximate term scheme for the haloethenes, C_2F_3H, C_2F_3Cl and $C_2F_2Cl_2$ based on the energies and symmetries of the orbitals derived by photoelectron spectroscopy [7–10]. The positions of the π^*, σ_{Cl}^* and Rydberg orbitals comes from the absorption data [3–5], and the present fluorescence studies. Indicative transitions from the inner valence orbitals are shown, together with the first members of the observed Rydberg series that converge to the first ionisation potentials and all the Rydberg transitions that are observed converging to the second ionisation potentials. The wavelengths of the transitions (in nm) are given for the transitions.

spectra in this region rather than the present fluorescence excitation spectra might yield additional information.

A final comment concerns the identification of the emitters in the fluorescence excitation spectra. The assignment of the emission to electronically-excited CF_2^* or CXY^* has been achieved by a crude characterisation of its wavelength range. Whilst this is probably reasonable and correct for excitation wavelengths greater than ≈ 100 nm, it is by no means certain that the emitters remain electronically-excited halocarbene radicals for shorter wavelengths. It is clearly important that measurement of the dispersed fluorescence at a range of excitation wavelengths is undertaken to unambiguously identify the emitters. However, this is a technically challenging experiment given the weakness of synchrotron radiation as an excitation source. One interesting feature of this study is that these haloethenes possess such large quantum yields for fluorescence at energies that greatly exceed the energies required for ionisation. One might expect that fluorescence would decrease above the ionisation threshold as the quantum yield for ionisation rapidly approaches unity.

Acknowledgements

We gratefully acknowledge support of this work by the EPSRC.

References

[1] A.J. Merer, R.S. Mulliken, Chem. Rev 69 (1969) 639.
[2] R.B. Robin, Higher Excited States of Polyatomic Molecules, Vol. 3, Academic Press, Orlando, 1985.
[3] J.D. Scott, R.D. Russell, Chem. Phys. Lett. 9 (1971) 375.
[4] B.R. Scott, B.R. Russell, J. Am. Chem. Soc. 94 (1972) 2634.
[5] G. Bélanger, C. Sandorfy, J. Chem. Phys. 55 (1971) 2055.
[6] J.B. Nee, X. Wang, M. Suto, L.C. Lee, Chem. Phys. 113 (1987) 265.
[7] R.F. Lake, H. Thompson, Proc. Royal Soc. London A 315 (1970) 323.
[8] J.A. Sell, A. Kuppermann, J. Chem. Phys. 71 (1979) 4703.
[9] G. Bieri, W. Von Niessen, L. Åsbrink, A. Svensson, Chem. Phys. 60 (1981) 61.
[10] A.W. Potts, J.M. Benson, I. Novak, W.A. Svensson, Chem. Phys. 115 (1987) 253.
[11] M.J. Coggiola, W.M. Flicker, O.A. Mosher, A. Kuppermann, J. Chem. Phys. 65 (1976) 2655.
[12] C.J. Apps, M.J. Bramwell, J.L. Cooper, J.C. Whitehead, F. Winterbottom, Molec. Phys. 83 (1994) 1265.
[13] G. Tornow, R. Locht, R. Kaufel, H. Baumgärtel, H.W. Jochims, Chem. Phys. 146 (1990) 115.
[14] E. Rühl, H.W. Jochims, H. Baumgärtel, Can. J. Chem. 63 (1985) 1949.
[15] R.E. Huie, N.J.T. Long, B.A. Thrush, Chem. Phys. Lett. 51 (1977) 192.
[16] T. Ibuki, A. Hiraya, K. Shobatake, J. Chem. Phys. 90 (1989) 6290.
[17] T. Ibuki, A. Hiraya, K. Shobatake, Y. Matsumi, M. Kawasaki, J. Chem. Phys. 92 (1990) 4277.
[18] M. Ahmed, C.J. Apps, C. Hughes, J.C. Whitehead, J. Phys. Chem. 98 (1994) 12530.
[19] C.Y.R. Wu, T.J. Xia, G.S. Liu, R. McDiarmid, J. Chem. Phys. 94 (1991) 4093.